Multiscale Models of Sweep Gas and Porous Support Effects on Zeolite Membranes

Anastasios I. Skoulidas
National Energy and Technology Laboratory, Pittsburgh, PA 15236

David S. Sholl
Dept. of Chemical Engineering, Carnegie Mellon University, Pittsburgh, PA 15213
and
National Energy and Technology Laboratory, Pittsburgh, PA 15236

DOI 10.1002/aic.10335
Published online in Wiley InterScience (www.interscience.wiley.com).

Existing detailed models of gas permeation through zeolite membranes have focused on adsorption and diffusion within zeolite crystals. Practical zeolite membranes, however, are typically grown as thin films on porous supports and are often studied experimentally in the presence of a sweep gas in addition to the permeating species of interest. We have used a combination of atomically detailed and continuum models to examine the impact of sweep gases and porous supports on permeation of CH_4 through silicalite membranes at room temperature. The adsorption and transport properties of the gas mixture inside the zeolite are treated using atomically detailed models, whereas transport in the porous support is treated using well-validated continuum models. Our results indicate that the effect of He as a sweep gas on unsupported membranes is minor. In many cases, the use of a porous support when no sweep gas is present also has only negligible effects compared to that of an unsupported membrane. When a sweep gas and a porous support are present, however, strong deviations from the permeation properties of an equivalent unsupported membrane with no sweep gas can occur, and these effects can depend strongly on whether the support faces the feed or permeate side of the process. These observations are related to existing experimental studies of gas permeation through zeolite membranes. © 2005 American Institute of Chemical Engineers *AIChE J,* 51: 867–877, 2005

Keywords: computational chemistry (kinetics/thermo), membrane separations, membrane materials, zeolites, multiscale simulations

Introduction

Membranes made from thin films of zeolites have been extensively studied as attractive devices for gas- and liquid-phase separations. For reviews of this field, see Matsukata and Kikuchi,[1] Coronas and Santamaria,[2] and Tsapatsis and Gavalas.[3] Because they are composed of crystalline inorganic materials, zeolite membranes can be used in a broad range of temperatures, pressures, and chemical environments. In addition to their chemical and thermal stability, zeolites are attractive as membrane materials because of their atomically ordered nanometer-scale pore structures. Because of the strong confinement of molecules inside the zeolite pores, the adsorption and transport properties of molecules adsorbed in zeolites can vary enormously as functions of such parameters as pore size, adsorbate size and shape, and temperature.[4,5] These variations

Correspondence concerning this article should be addressed to D. S. Sholl at sholl@andrew.cmu.edu.

© 2005 American Institute of Chemical Engineers

are one of the key factors in making zeolites useful as membrane materials.

Practical zeolite membranes are typically composite membranes, with zeolite thin films grown on tubular or flat porous supports such as porous steel or α-alumina.[2,3,6] These supports provide mechanical strength to the membrane but are intended to introduce minimal transport resistances. Studies of a variety of supported membranes have shown that the resistance introduced by porous supports cannot always be neglected. For example, the permeance of supported membranes is known to depend on whether the membrane layer faces the feed side or the permeate side.[6-8] Gas transport through porous supports can involve multiple transport mechanisms, so the net support resistance can vary in a complex way with process conditions.[9-11]

The permeance of gas species through zeolite membranes can be probed in a variety of experiments.[6] Single-component permeance can be easily assessed in experiments that impose a constant pressure drop across a membrane. In many experiments, however, a sweep gas is used on the membrane's permeate side to create a partial pressure drop in the permeating species while reducing or eliminating the total pressure drop across the membrane.[6,7,12,13] Comparisons between these two classes of experiments have indicated that the presence of sweep gases can have a substantial impact on the absolute flux of the permeating species and that the strength of this effect is dependent on the identity of the sweep gas.

We have recently shown that atomically detailed calculations can be used to quantitatively predict the single-component flux of light gases such as CH_4 and CF_4 through zeolite membranes.[14] In our approach, atomistic simulations are used to determine the adsorption isotherms and loading-dependent Fickian diffusion coefficient, $D_t(c)$. These results are then used to solve a macroscopic description of permeance through an unsupported zeolite membrane. We have also applied this approach to the permeation of binary gas mixtures through zeolite membranes.[15] We previously argued that this approach holds a number of advantages compared to those of other means for predicting membrane permeance using either direct atomistic simulations of nonequilibrium transport or using empirical models parameterized from experimental data.[14,16,17]

The aim of this article is to extend our previous atomically detailed models of gas permeation through zeolite membranes to systematically study the influence of support resistance, membrane orientation, and sweep gases on the permeation of light gases through supported zeolite membranes. In particular, we examine membranes at room temperature with CH_4 as a permeating gas and He as a sweep gas. By examining various physical configurations in order of increasing complexity, our model provides insight into the roles of the factors that contribute to the overall performance of supported membranes.

We begin by examining the effect of He as a sweep gas on CH_4 permeance through unsupported silicalite membranes. This situation is modeled with full atomistic detail by determining the binary transport diffusion coefficients and adsorption isotherms from atomistic simulations, following our previous work.[15,17-20] In addition to giving useful information for analyzing more complex situations involving supported membranes, there have been experimental studies of unsupported zeolite membranes that used He as a sweep gas.[13] Analysis of these experiments has typically assumed that He is nonadsorbing, which implies that the experiments can be treated as single-component permeance. Our model allows the validity of this assumption to be examined.

The second configuration we examine is that of a zeolite membrane supported on a porous support operated without the presence of a sweep gas. In this situation it is not appropriate to apply atomically detailed methods to describe gas transport in the porous support, so a combination of existing continuum methods are used to describe the combined effects of viscous flow and Knudsen diffusion in the support. These methods are combined with information from atomistic descriptions of the zeolite layer to give information on the overall permeance of CH_4 through the supported membrane. This model is used to examine the influence of the support properties and also the orientation of the asymmetric membrane with respect to the feed on the overall permeance.

After separately examining the influence of a sweep gas and support layers, we use our model to examine the impact of using a sweep gas with a supported membrane. In this case, molecular diffusion of the gas species in the porous support must also be considered, so the continuum models of the porous support are extended to include this phenomenon. Again, the model is used to examine the role of membrane orientation with respect to the feedstream.

Effect of He Sweep Gas on CH_4 Permeance through Unsupported Membranes

The first and simplest membrane configuration we consider is an unsupported single crystal silicalite membrane, which we will refer to as the *bare membrane*. We have used atomically detailed models of CH_4 and He adsorption and diffusion in silicalite to examine how using He as a sweep gas in membranes of this type affects CH_4 permeance. All calculations in this section were for a membrane operating at room temperature. The details of our atomistic models for single-component adsorption and transport have been described elsewhere,[18-20] and herein we used the same intermolecular potentials for CH_4 and He as in our earlier work. Cross-species potentials were defined by the Lorenz–Berthelot combination rules from the pure species potentials. We previously demonstrated how atomistic simulations can be used to rigorously describe transport of CH_4/CF_4 mixtures in silicalite.[15]

In the present work, we have applied atomistic simulation methods to CH_4/He mixtures in silicalite at room temperature. To fully describe macroscopic transport, the binary adsorption isotherm and loading-dependent transport diffusion coefficients must be known. We computed the room temperature binary adsorption isotherm using grand canonical Monte Carlo (GCMC) simulations.[15,21-26] The chemical potential of each component in the bulk gas mixture was related to the partial pressures by a virial equation of state using experimentally determined second virial coefficients for CH_4[27] and He.[28] To obtain adsorption data spanning the full range of possible adsorbate compositions, GCMC simulations were used to determine the adsorbed amount corresponding to bulk gas compositions varying from 0 to 100% CH_4 and total bulk pressures up to 100 bar. To use our calculated binary adsorption isotherm in conjunction with the macroscopic model described above, it is necessary to fit the calculated data to a continuous function. We did this with the following empirical function

Table 1. Parameters for the Binary Adsorption Empirical Isotherms of Eq. 1*

Parameter	Value	Parameter	Value
a_1	7.99243	b_1	0.056702
a_2	0.835765	b_2	0.001557
a_3	0.001341	b_3	0.000124
a_4	2.455041	b_4	3.460191
a_5	6.929885	b_5	0.13345
a_6	0.862249	b_6	0.799613
a_7	0.02647	b_7	0.002951
a_8	5.123772	b_8	2.799088

*Parameters a_1, a_5, b_1, and b_5 have units of molecules per unit cell. Parameters a_4, a_8, b_4, and b_8 have the units of pressure (bar). Other parameters are dimensionless.

$$\left.\begin{aligned} c_1 &= \frac{a_1 P_1}{a_2 P_1 + a_3 P_2 + a_4} + \frac{a_5 P_1}{a_6 P_1 + a_7 P_2 + a_8} \\ c_2 &= \frac{b_1 P_2}{b_2 P_1 + b_3 P_2 + b_4} + \frac{b_5 P_2}{b_6 P_1 + b_7 P_2 + b_8} \end{aligned}\right\} \quad (1)$$

where c_i is the concentration in the zeolite and P_i is the bulk partial pressure of species i. Here and throughout the remainder of this paper, the subscripts 1 and 2 on concentrations, partial pressures, and so forth denote CH_4 and He, respectively. The coefficients that give the best fit are shown in Table 1. The average relative error between the fit and the calculations was less than 6%.

When using atomically detailed methods to simulate molecular diffusion in zeolites, it is convenient to describe macroscopic transport of binary mixtures using the Onsager description[29-31]

$$\begin{bmatrix} J_1 \\ J_2 \end{bmatrix} = -\begin{bmatrix} L_{11} & L_{12} \\ L_{21} & L_{22} \end{bmatrix} \begin{bmatrix} \partial \mu_1 / \partial s \\ \partial \mu_2 / \partial s \end{bmatrix} \quad (2)$$

where s is the transmembrane direction; and L_{ij}, the Onsager coefficients, are functions of the adsorbate concentrations and form a symmetric matrix. The Onsager coefficients can be determined directly from equilibrium molecular dynamics (EMD) simulations.[15,31-33]

We computed the Onsager transport coefficients using the same methods as in our previous work on CH_4/CF_4 mixtures in silicalite.[15] Diffusion in silicalite is anisotropic,[34] but for simplicity we have used orientationally averaged diffusivities and transport coefficients throughout this paper. Using orientationally averaged diffusivities is appropriate for making comparisons with membranes composed of randomly oriented crystals.[14,15] Examples of the Onsager coefficients from our calculations are illustrated in Figure 1, which shows the three independent Onsager coefficients (L_{11}, L_{22}, and L_{12}) as a function of the total concentration in silicalite for CH_4/He mixture that is 90% CH_4. As above, the subscripts 1 and 2 denote CH_4 and He, respectively. One important observation that becomes evident from this figure is that the off-diagonal Onsager coefficients L_{12} can be comparable in magnitude to the diagonal transport coefficients, particularly when the total adsorbed concentration in the zeolite is large. This observation has been made before for CH_4/CF_4 mixtures in silicalite[14] and it shows that the approximation of treating the off-diagonal Onsager coefficients as zero[35-41] may often be inaccurate.

As with our GCMC calculations, we need to fit the Onsager coefficients determined from our EMD calculations to a continuous function to use it in a macroscopic model. We evaluated the matrix of Onsager coefficients using EMD for a large grid of mixture compositions corresponding to total bulk pressures up to 100 bar. We fitted the resulting data using the same empirical expressions we used previously to fit the Onsager coefficients of CH_4/CF_4[15]

$$L_{11} = d_1 a_1^{(b_1 - n_1)^2/c_1} a_2^{(b_2 - n_2)^2/c_2} n_1 \quad (3)$$

$$L_{22} = d_2 a_3^{(b_3 - n_1)^2/c_3} a_4^{(b_4 - n_2)^2/c_4} n_2 \quad (4)$$

$$L_{12} = L_{21} = d_3 a_5^{(b_5 - n_1)^2/c_5} a_6^{(b_6 - n_2)^2/c_6} n_1 n_2 \quad (5)$$

Here, n_i is the concentration of species i in the zeolite expressed in molecules per unit cell. The resulting parameters for Eqs. 3–5 are listed in Table 2.

The Onsager formulation of binary transport, Eq. 2, is just one of several well-known descriptions of multicomponent diffusion. The Maxwell–Stefan and Fickian formulations of multicomponent diffusion are also convenient in many instances.[29,42] From a formal perspective, these differing formulations are equivalent because once the relevant diffusivities or transport coefficients are specified for one formulation then the other formulations are also fully defined.[29,43] We found it convenient to use a Fickian description of binary transport for numerical calculations with practical membrane configurations

$$\begin{bmatrix} J_1 \\ J_2 \end{bmatrix} = -\begin{bmatrix} D_{11} & D_{12} \\ D_{21} & D_{22} \end{bmatrix} \begin{bmatrix} \partial c_1 / \partial s \\ \partial c_2 / \partial s \end{bmatrix} \quad (6)$$

The loading-dependent Fickian diffusivities, $D_{ij}(c_1, c_2)$, can be calculated without approximation from the binary adsorption isotherm, Eq. 1, and the Onsager transport coefficients, Eqs. 3–5.[29,43]

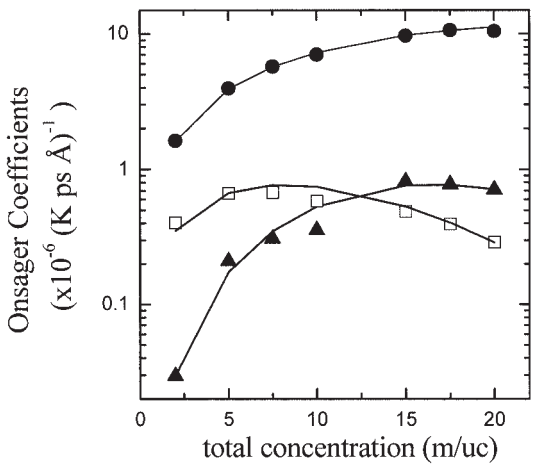

Figure 1. Onsager coefficients for a CH_4/He mixture that is 90% CH_4. L_{11} (filled circles), L_{22} (filled triangles), and L_{12} (open squares), with 1 for CH_4 and 2 for He, are measured in ps^{-1}Å^{-1} K^{-1}.

The solid lines are the empirical fits given by Eqs. 3–5.

Table 2. Parameters for the Empirical Functions of Eqs. 3–5*

Parameter	Value	Parameter	Value	Parameter	Value
a_1	1.0233	b_1	0.507483	c_1	29.05549
a_2	1.089877	b_2	−7.446784	c_2	22.50037
a_3	1.06713	b_3	−7.679634	c_3	15.66798
a_4	0.999393	b_4	3.445537	c_4	0.036044
a_5	2.03794	b_5	−1.505739	c_5	168.5784
a_6	1.019984	b_6	2.047714	c_6	0.49933
d_1	1.119753	d_2	2.142474	d_3	0.098737

*Parameters d_i have units of molecules ps^{-1} $Å^{-1}$ K^{-1}. Other parameters are dimensionless.

To assess the effect of the sweep gas on the permeance of CH_4 through the bare membrane we have compared the room temperature CH_4 fluxes through a 100-μm silicalite membrane with and without He as a sweep gas. Pure CH_4 fluxes were calculated by a straightforward integration of Fick's law of diffusion for a single species.[14,17] The transport diffusivity of pure CH_4 using the atomistic model described above was previously calculated.[18,19] CH_4 fluxes under the presence of He were calculated by solving Eq. 6 using the numerical method of lines,[44] with the loading-dependent Fickian diffusivities calculated as described above. For the boundary conditions of the binary mixture calculation, it was assumed that the total pressure at the feed side and the permeate side were equal. The feed was a CH_4/He mixture with a CH_4 concentration that varied from 0.5 to 99%, whereas the permeate side consisted of pure He. In the pure CH_4 calculations the feed pressure was equal to the partial pressure of CH_4 in the mixtures with He, whereas the permeate side was kept at zero pressure. In Figure 2 we show the relative percentage difference between the pure CH_4 fluxes and the fluxes with the sweep gas, as a function of CH_4 concentration and the total feed pressure. It is clear from Figure 2 that, although the presence of the sweep gas does have an effect on the CH_4 fluxes through the bare zeolite membrane, the overall effect is negligible. The impact of the sweep gas is greatest, as might be expected, when the total pressure is large and the CH_4 partial pressure in the feed is small.

For very low CH_4 partial pressures, Figure 2 suggests that the sweep gas may slightly increase the permeation rate relative to that of a pure single-component system. This prediction is an artifact of the fitting functions used in Eqs. 3–5. In this limit, Eqs. 3–5 slightly overestimate L_{11} and underestimate L_{12}, with the net result that the Fickian diffusivities of CH_4 are slightly overestimated.

Talu et al.[13] measured the diffusivities of *n*-alkanes through single-crystal silicalite membranes using He as a sweep gas. In most of their experiments the pressure of pure He at the permeate side was larger than the inlet pressure of the He/*n*-alkane mixture at operating pressures lower than 15 torr. Our calculations suggest that under these conditions the effect of He on the measured diffusivities should be less than 1%. These results provide additional justification for the assumptions made by Talu et al.[13] In some experiments,[45] a heavier inert gas such as Ar has been used as a sweep gas. In these cases the influence of the sweep gas will be stronger than when using He as a sweep gas. This effect has been demonstrated in the case of supported membranes by van der Graaf et al.[6,7]

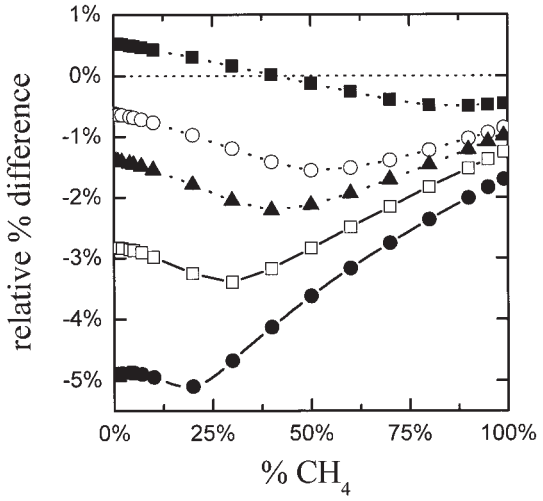

Figure 2. Relative percentage difference between CH_4 fluxes through an unsupported silicalite membrane at 298 K, with and without He as a sweep gas, for feed pressures of (in kPa) 296 (■), 502 (○), 640 (▲), 900 (□), and 1280 (●).

Negative values denote a reduction of CH_4 flux attributed to the sweep gas.

Effect of Porous Support on CH_4 Permeance through Supported Membranes

Practical zeolite membranes typically have a thin zeolite layer grown onto a porous support. In this section, we present a model for the flow of pure CH_4 through a porous support and combine this model with the atomistic description given above of CH_4 permeance through silicalite to examine the impact of supports on net permeance. The atomistic details for describing single-component permeation of CH_4 through silicalite at a range of temperatures were taken from our earlier work.[14,15,18,19] Rather than attempt to describe gas flow through a porous support from atomistic principles, we adopt a continuum model. The support can be placed at the permeate side (normal position) or on the feed side (reverse position). Below we examine both of these configurations to examine the influence of the support position.

We model the support as having thickness L_s and being formed from an array of straight and parallel pores with radius r_p and porosity/tortuosity ratio ε/τ. Flow of a single component fluid through such a support can be described as a combination of Knudsen and viscous flow. Knudsen flow, which occurs in the limit where the mean free path is much larger than the pore diameter, $\lambda \gg 2r_p$, gives a molecular flux N_k of[46,47]

$$N_k = -\frac{D_k}{RT}\frac{dP}{ds} \tag{7}$$

Here, P is the pressure, s is the direction of the flow through the tube, R is the gas constant, and T is temperature. The Knudsen diffusivity D_k for a species with molecular weight MW is

$$D_k = \frac{2r_p}{3}\sqrt{\left(\frac{8RT}{\pi MW}\right)} \tag{8}$$

When the mean free path is much smaller than the pore diameter, $\lambda \ll 2r_p$, a continuum fluid description is appropriate. The molecular flux in this case is

$$N_c = -\frac{1}{RT}\left[\frac{r_p^2 P}{8\mu} + u_0\right]\frac{dP}{ds} \tag{9}$$

where μ is the kinematic viscosity and u_0 is the slip velocity at the pore wall. At high pressures or for large pores where the slip velocity is negligible, this expression reduces to the well-known Poiseuille flow.

There is a large body of work that has explored various means to describe the transition between Eqs. 7 and 9.[46-53] We have used a description developed by Datta and Rinker that gives accurate predictions for gas flow over a wide range of pressures and pore widths.[46] With this description, the molecular flux is expressed by

$$N_k = -\frac{D_T}{RT}\frac{dP}{ds} \tag{10}$$

with

$$D_T = \phi_K D_K + (1-\phi_K)\left[\frac{r_p^2 P}{8\mu\Phi} + \frac{3\pi}{18}D_K\right] \tag{11}$$

Here, ϕ_K is the fraction of molecules that does not experience any intramolecular collisions between two successive collisions with the wall and Φ is the ratio of the transition viscosity to the continuum viscosity. By introducing the Knudsen number, $K_I = 2r_p/\lambda$, and a geometrical factor b, which for an infinitely long tube has the value of 0.81, ϕ_K and Φ are defined by

$$\phi_K = e^{-bK_I} \tag{12}$$

and

$$\Phi = 1 - bK_I\frac{e^{-bK_I}}{1-e^{-bK_I}} = 1 - bK_I\frac{\phi_K}{1-\phi_K} \tag{13}$$

When applied to a porous support with a porosity/tortuosity ratio of ε/τ, Eq. 10 becomes

$$N_k = -\frac{D_T^{\text{eff}}}{RT}\frac{dP}{ds} \tag{14}$$

Table 3. Dimensionless Parameters for the Viscosity Collision Integral*

A	1.16145	D	0.77320
B	0.14874	E	2.16178
C	0.52487	F	2.43787

*Adapted from Reid et al.[54]

where the effective diffusivity is

$$D_T^{\text{eff}} = \frac{\varepsilon}{\tau}D_T \tag{15}$$

To apply the description above, the mean free path and kinematic viscosity must be given as functions of pressure. The mean free path is[54]

$$\lambda = \frac{1}{\sqrt{2}}\frac{k_B T}{\pi P\sigma^2} \tag{16}$$

where k_B is the Boltzmann constant and σ is the collision diameter. The kinematic viscosity was calculated by the method of Chung et al.[55]

$$\mu = 40.785\frac{F_c\sqrt{MW\cdot T}}{V_c^{2/3}\Omega_v} \tag{17}$$

where Ω_v is the collision integral,[54] V_c is the critical volume, and for nonpolar species $F_c = 1 - 0.2756\omega$, where ω is the acentric factor. Equation 17 yields μ in μP when MW is measured in g/mol and V_c is measured in cm^3/mol. If the interaction between the gas molecules is given by a Lennard–Jones potential, then Ω_v can be calculated.[54] A fit to such calculations is given by

$$\Omega_v = A(T^*)^{-B} + Ce^{-DT^*} + Ee^{-FT^*} \tag{18}$$

where $T^* = k_B T/\varepsilon_u$ is a reduced temperature with ε_u the Lennard–Jones interaction energy. For Chung's method $\varepsilon_u/k_B = T_c/1.2593$, where T_c is the critical temperature measured in Kelvin, and $\sigma = 0.809V_c^{1/3}$. The same σ was used in Eq. 16. The constants in Eq. 18 are given in Table 3.

We note that the preceding model must break down for sufficiently small pores. Recent work by Bhatia et al.[56] has carefully explored this phenomenon. The majority of the calculations below are for pores in the support material of diameter 250 nm. This width is certainly sufficient for the macroscopic model described above to be applied with confidence.

The combined membrane/support problem was solved with the numerical method of lines.[44] With this method the time-dependent equations of diffusion were integrated to a steady state. The feed pressure was varied from 121 to 1600 kPa, whereas the permeate pressure was set to zero. The support and the membrane diffusion equations were solved independently, coupled only through the boundary conditions at the support/membrane interface. We used this methodology to study the effect of the characteristics of the support, such as pore radius, thickness and porosity/tortuosity ratio, the temperature, and the support position on the fluxes of CH_4 through a silicalite

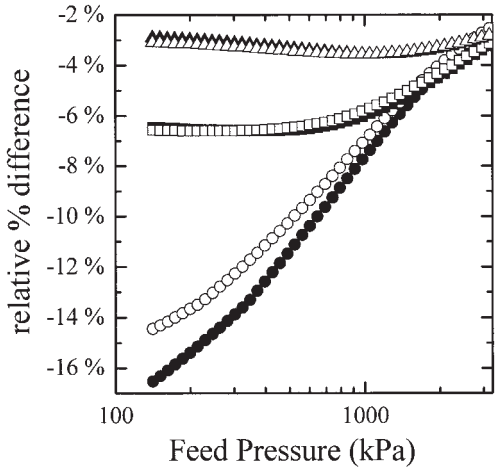

Figure 3. Relative percentage difference between CH_4 fluxes through an unsupported and supported silicalite membrane at 298 (●, ○), 373 (■, □), and 473 K (▲, △) and configurations with the support downstream (closed symbols) and upstream (open symbols).

The support has a thickness of 1590 μm, ε/τ ratio of 0.27, and pore radius of 250 nm. The silicalite membrane is 140 μm thick.

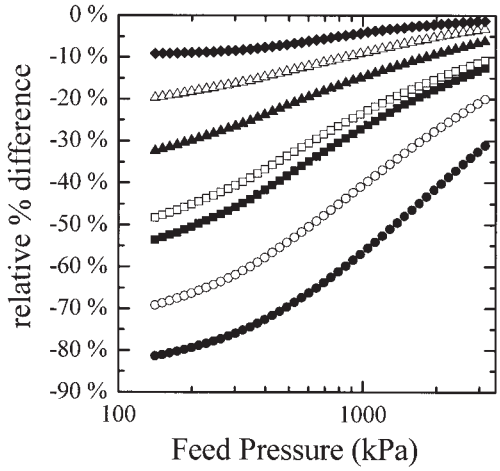

Figure 4. Similar to Figure 3 for a downstream support with the same thickness and ε/τ ratio but with a pore radius of (in nm) 10 (●), 20 (○), 40 (■), 50 (□), 100 (▲), 200 (△), and 500 (♦).

membrane. To study the effect of the temperature and the support placement we chose to model a support with a thickness of 1590 μm, an ε/τ ratio equal to 0.27, and a pore radius of 250 nm. These parameters correspond to a porous steel support used in the experiments of Bowen et al.[14] For the rest of the paper we refer to this support as the *porous steel support*. To facilitate a comparison with our previous results[14] we have modeled a silicalite membrane that is 140 μm thick.

In Figure 3 we show the percentage flux reduction of CH_4 resulting from the porous steel support as a function of temperature for the normal and reverse support positions (closed and open symbols in Figure 3, respectively). In all cases the support acts as an extra resistance, reducing CH_4 flux through the silicalite membrane. At lower temperatures and feed pressures we see a difference between the two support positions, with the normal support position exhibiting a larger resistance than that of the reverse position. These effects are diminished at higher temperatures and feed pressures. At 473 K the reduction attributed to the support is less than 2% for all feed pressures. Differences in the support resistance between the normal and the reverse position for pure gas permeation have been observed experimentally for hydrocarbon permeation through a silicalite membrane.[6]

We used the conditions showing the largest support resistance in Figure 3, that is, the normal support position at room temperature, to explore the effect of the support characteristics on CH_4 fluxes. In Figure 4 we show the percentage CH_4 flux reduction as a function of the support's pore size. As would be expected, as the pore size is decreased the resistance to transport through the support increases. In the narrowest of these pores, it is likely that deviations from the macroscopic model we used to define the resistance to transport may exist, as suggested by studies of transport through very small pores.[56] The resistance to transport through the support also increases when the support's thickness is increased (Figure 5) or when the support's porosity/tortuosity ratio is decreased (Figure 6). In all cases, the largest support resistance is experienced at low feed pressures.

The difference between the two support positions shown in Figure 3 can be explained based on the shape of CH_4 isotherm as a function of the pressure (Figure 7). At room temperature the adsorption of CH_4 in silicalite is strong and the slope of the isotherm is large at low pressures. At higher pressures the slope of the isotherm is greatly reduced. As a result, the small pressure drop attributed to the support causes a smaller concentration drop on the zeolite layer at the normal position than that at the reverse position. At higher temperatures the adsorption isotherms are more linear over the same range of pressures, so the difference between the two support positions

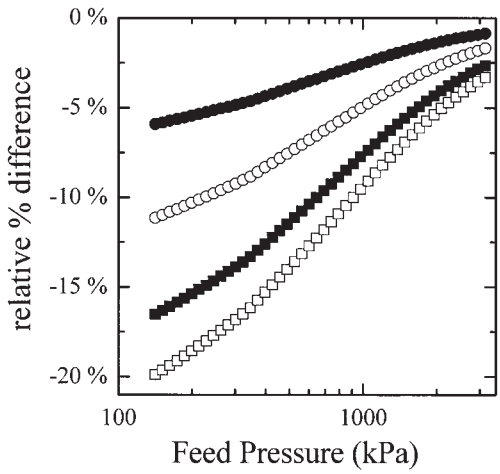

Figure 5. Similar to Figure 3 for a downstream support with the same pore radius and ε/τ ratio but with a thickness of (in μm) 500 (●), 1000 (○), 1590 (■), and 2000 (□).

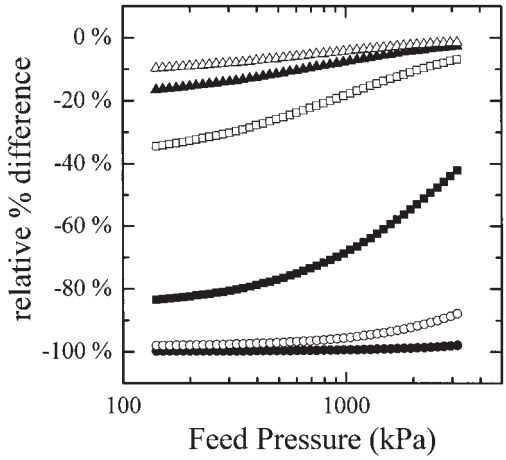

Figure 6. Similar to Figure 3 for a support with the same thickness and pore radius but with an ε/τ ratio of 0.0001 (●), 0.001 (○), 0.01 (■), 0.1 (□), 0.27 (▲), and 0.5 (△).

diminishes. This has also been demonstrated in experiments by van de Graaf et al.[6]

Previously, we used the unsupported zeolite membrane model to predict the flux of CH_4 through a silicalite membrane at various temperatures as a function of the feed pressure.[14] These predictions were in good agreement with the experimental measurements.[14] In those calculations the thickness of the membrane was fitted to the room temperature measurements; the fitted thickness was 140 μm. In these experiments the silicalite membrane was grown on a porous steel support and the membrane was operated with the support on the downstream side.[14] The thickness of that membrane was experimentally determined to be on the order of 100 μm.[14] We reanalyzed those results with the supported membrane model described above, which specifies the physical characteristics of the support. The thickness of the silicalite membrane was again fitted to the room-temperature measurements, the results of which are shown in Figure 8. The points in Figure 8 are the experimentally measured CH_4 permeance at 298 and 373 K. The

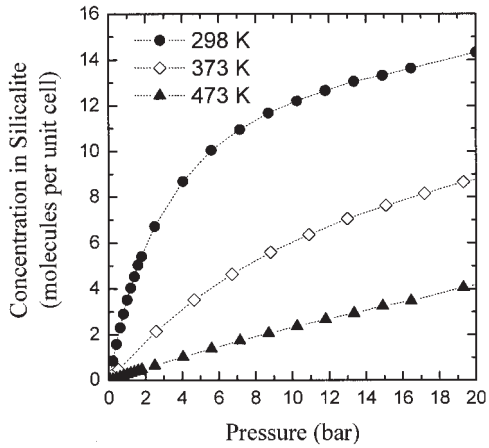

Figure 7. Adsorption isotherm of CH_4 in silicalite at room temperature as a function of the bulk gas pressure.

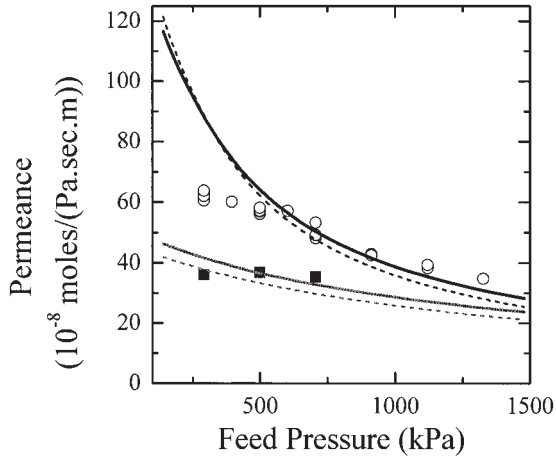

Figure 8. Permeance of CH_4 through a silicalite membrane.

The points are experimental data from Bowen et al.[14] for 298 (○) and 373 K (■). The dashed lines are predictions of the permeance through an unsupported silicalite membrane 140 μm thick. The solid lines are predictions of the permeance through a supported silicalite membrane as described in the text.

dashed lines represent the calculated permeance for the unsupported silicalite membrane based on a 140-μm-thick zeolite layer. The solid lines are the predictions using the supported membrane model with the porous steel parameters for the support. When the support is included, the fitted thickness of the silicalite membrane is 118 μm. Comparing the unsupported and supported model results in Figure 8 suggests that the support does not change the characteristics of CH_4 transport, so predictions of the unsupported membrane model have the same level of accuracy when an effective zeolite thickness is used.

Combined Effects of Porous Support and He Sweep Gas on CH_4 Permeance

We have earlier considered separately the effects of He as a sweep gas and a porous support. In this section, we consider the combined effects of these two approaches; that is, the impact of using a sweep gas on a zeolite membrane grown on a porous support. This situation can be described by the models developed above, provided that our description of flow through the porous support is augmented to account for the flow of a binary mixture. To make this extension, we used the dusty gas model (DGM).[57,58] The DGM has been successfully applied to a number of other examples of binary gas diffusion through composite membranes.[9-11]

In cases where a total pressure gradient exists, the DGM for a binary mixture is[57,58]

$$\frac{N_i}{D_{iK}} + \sum_{i \neq j} \frac{x_j N_i - x_i N_j}{D_{12}} = -\frac{dc_i}{dz} - \frac{x_i P B_0}{\mu_{12} D_{iK}} \frac{dc_i}{dz} \qquad i = 1, 2 \quad (19)$$

where c_i is the concentration of species i; c_t is the total concentration; N_i represents the molecular fluxes; x_i represents the mole fractions; D_{12} is the molecular diffusion coefficient; D_{iK} is the Knudsen diffusion coefficient for species i; μ is the kinematic viscosity for the mixture; and B_0 is a shape factor,

which for a long cylindrical capillary has the value $r_p^2/8$. The Knudsen diffusion coefficients are given by Eq. 8. The mixture kinematic viscosity was calculated using Chung's method,[55] which uses a corresponding-states approach to calculate the mixture parameters from the critical parameters of the pure components. More details about this method are given in Reid et al.[54] The molecular diffusivity was calculated with a correlation given by Reid et al.[54]

$$D_{12} = \frac{0.00143T^{1.75}}{P\sqrt{MW_{12}}[(\Sigma_u)_1^{1/3} + (\Sigma_u)_2^{1/3}]^2} \tag{20}$$

measured in cm^2/s, where P is the total pressure; T is the temperature; Σ_u is the molecular diffusion volume, which is a parameter fitted to experimental data[59]; and $MW_{12} = 2(MW_1^{-1} + MW_2^{-1})^{-1}$.

Equation 19 can be rearranged to give

$$N_i = -D_{iA}\frac{dc_i}{dz} - D_{iB}\frac{dc_t}{dz} \qquad i = 1, 2 \tag{21}$$

with

$$D_{iA} = \frac{D_{12}D_{iK}}{D_{12} + x_2D_{1K} + x_1D_{2K}}$$

and

$$D_{iB} = \frac{x_iD_{1K}D_{2K}}{D_{12} + x_2D_{1K} + x_1D_{2K}} + \frac{x_iPB_0}{\mu_{12}} \qquad i = 1, 2 \tag{22}$$

For a support with a porosity and tortuosity ratio of ε/τ the diffusion coefficients D_{iA} and D_{iB} are replaced by the effective transport coefficients defined by Eq. 15.

When there is no gradient in the total pressure, Eq. 19 simplifies to

$$-\frac{dc_i}{dz} = \frac{\chi_2N_1 - \chi_1N_2}{D_{12}^e} + \frac{N_1}{D_{iK}^e} \qquad i = 1, 2 \tag{23}$$

This expression can be rearranged to give expressions for the molecular fluxes of each species analogous to Eq. 22. Equation 23 is appropriate for modeling the Wicke–Kallenbach method[6,7] for measuring the permeation of gases.

To examine the combined presence of a sweep gas and a membrane support, the dusty gas model described earlier was used for the porous support, whereas the atomistic description developed above for CH_4/He mixtures was used in the zeolite layer. All of the calculations below refer to membranes operating at room temperature. The combined transport equations for the zeolite layer and support were integrated numerically using the method of lines.

We first discuss examples in which no net pressure gradient exists across the membrane. We calculated the flux of CH_4 through a 100-μm-thick silicalite membrane supported by porous steel. The feed was a CH_4/He mixture of varying compositions and the permeate was pure He, both at total pressure P.

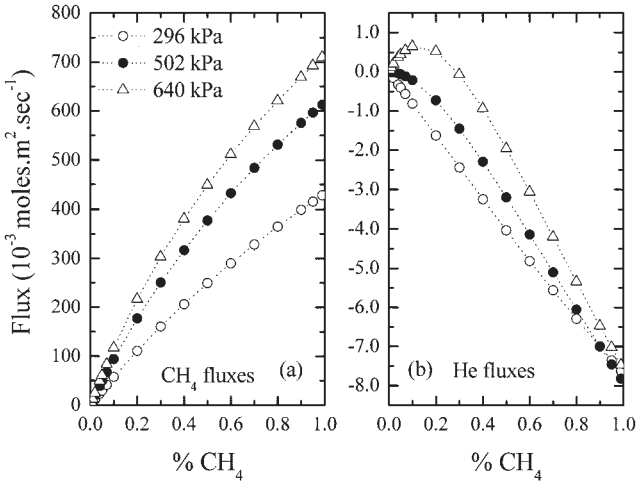

Figure 9. Fluxes of CH_4 (a) and He (b) through a supported silicalite membrane at isobaric conditions as a function of feed mixture concentration and system pressure.

The fluxes of CH_4 and He through the silicalite membrane are shown in Figure 9 as a function of the feed composition and P. In most cases the CH_4 and He fluxes are parallel to their respective concentration gradients. This situation is denoted by negative fluxes for He. For He-rich feeds and the highest pressures studied, however, we observed that He was flowing against its concentration gradient, as a result of the large off-diagonal diffusion coefficients and strong adsorption of CH_4. Using the bare membrane, with no sweep gas, as the reference state we calculated the reduction of CH_4 flux as a result of the presence of the sweep gas and the support. The calculations are summarized in Figure 10. Figure 10a shows

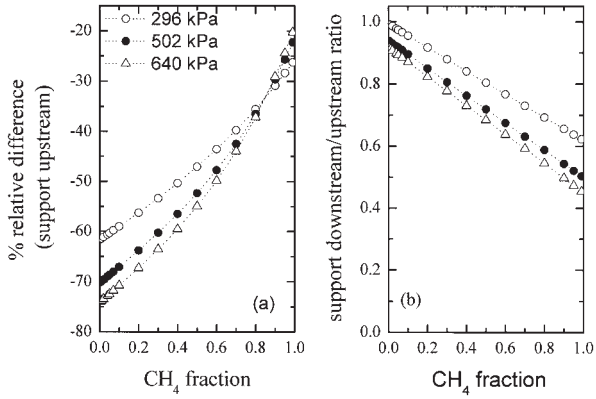

Figure 10. (a) Percentage reduction of CH_4 fluxes through a supported 100-μm silicalite membrane as a function of the feed composition and pressure when the support is placed upstream; (b) ratio of CH_4 fluxes through the downstream support/membrane configuration divided by the fluxes through the upstream support/membrane configuration as a function of the feed composition and pressure.

the percentage reduction in CH_4 fluxes as a function of the feed conditions for the reverse support position. The ratio of CH_4 fluxes between the two support positions is shown in Figure 10b. The magnitude of the reduction in CH_4 flux is striking when compared to the results above for a bare membrane with a sweep gas or a supported membrane with no sweep gas. The combination of a supported membrane and sweep gas can reduce the CH_4 flux by as much as 70%, with the strongest effects appearing for low CH_4 feed concentrations. The differences between the support positions are also striking. At high CH_4 concentrations, the flux of CH_4 is 50% less with the support in the normal position than that in the reverse support position.

Dramatic flux reductions arising from the combined presence of a membrane support and a sweep gas have been observed in permeation experiments of hydrocarbons through supported silicalite membranes with He as a sweep gas.[6,7] In those experiments, it was found that with the Wicke–Kallenbach (isobaric) method the flux of the hydrocarbons was substantially reduced for low partial pressures compared to the single gas-supported membrane-permeation experiments. At higher partial pressures the reduction was much smaller. The same trends are evident in our results. The physical origin of these effects is that the presence of the sweep gas in the support increases the effective pressure drop of CH_4 across the support layer, further reducing the concentration gradient of CH_4 across the zeolite layer relative to that of the bare membrane. This situation is enhanced with the support at the normal position.

Under isobaric conditions, transport in the support layer is dominated by molecular diffusion. This is not true in systems where a net pressure gradient exists because, in this case, Knudsen diffusion and viscous flow also occur in the support layer. We examined a variety of situations in which a net pressure gradient exists across a supported membrane in the presence of a sweep gas, using Eq. 19 to describe the support. Figure 11 shows the calculated flux through a supported membrane with and without He as a sweep gas in the feed. For calculations with the sweep gas, the total pressure of the feed was fixed at 298 kPa and the permeate pressure was assumed to be zero. In the calculations with no sweep gas, the permeate was once again held in a vacuum state, whereas the permeate pressure was set to the partial pressure of CH_4 in the corresponding sweep gas calculation. In complete contrast to the isobaric conditions described above, the combined presence of the support and the sweep gas changes the CH_4 flux in only a very minor way.

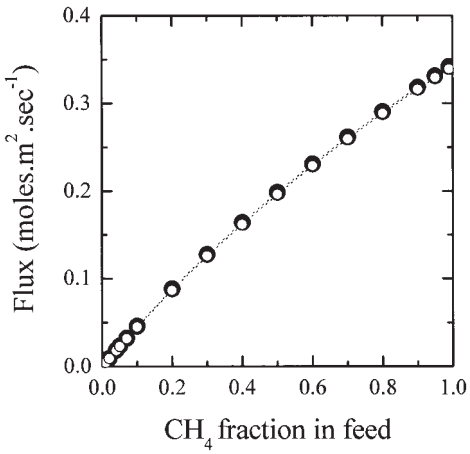

Figure 11. CH_4 fluxes through the supported silicalite membrane when there is a total pressure gradient with (closed symbols) and without (open symbols) He as a sweep gas on the feed side.

When a sweep gas is present the total feed pressure was 296 kPa. For the corresponding pure CH_4 calculations the pressure of the feed is equal to the partial pressure of CH_4 in its mixtures with He. In both cases the permeate side is held at vacuum.

Discussion and Conclusions

We have demonstrated how a combined atomistic–macroscopic modeling approach can be used to describe the transport of gas mixtures through supported zeolite membranes. Atomistic simulations have been used to parameterize a detailed macroscopic model of a gas mixture in the zeolite layer, whereas the support layer was modeled with a continuum approach that includes the combined effects of Knudsen diffusion, viscous flow, and molecular diffusion. The use of atomistic models to describe the properties of diffusing mixtures in the zeolite layer enables us to directly assess the impact of using a sweep gas in experiments that nominally examine the permeance of a single gas.

Our modeling approach was used to study the effects of the support layer on the transport of CH_4 through silicalite membranes, with and without He as a sweep gas. In many instances, it would be useful to compare the observed result from an unsupported membrane operated under truly single-component conditions, that is, with no sweep gas. Our calculations support the idea that under many conditions, the use of a porous support or the use of a sweep gas does not greatly alter the CH_4 flux relative to that of an unsupported membrane under single-component conditions. If an unsupported membrane is operated with He as a sweep gas, the sweep gas typically reduces the CH_4 flux by only a small amount compared to that of the single-component unsupported membrane. If CH_4 permeates as a single component through a supported membrane, a similar conclusion can be drawn. The resistance stemming from a porous support is of course a function of the thickness and porosity of the support, but under typical experimental conditions the net impact of the support relative to that of the unsupported membrane can be described as being small. The orientation of the supported membrane—that is, whether the support faces the permeate or feed side—does affect the absolute flux permeating through the membrane, but not dramatically.

There is one important example where the supported membrane gives results that are dramatically different from those of an unsupported membrane under single-component conditions: a supported membrane that is operated in conjunction with a sweep gas at isobaric conditions. Under these conditions, the impact of molecular diffusion in the binary gas mixture present in the porous support can be sizable, so the effective resistance presented by the support can be large. The CH_4 flux can be lowered by as much as 70% by the presence of a support and a He sweep gas relative to that of the single-component unsupported membrane. The differences between membrane ori-

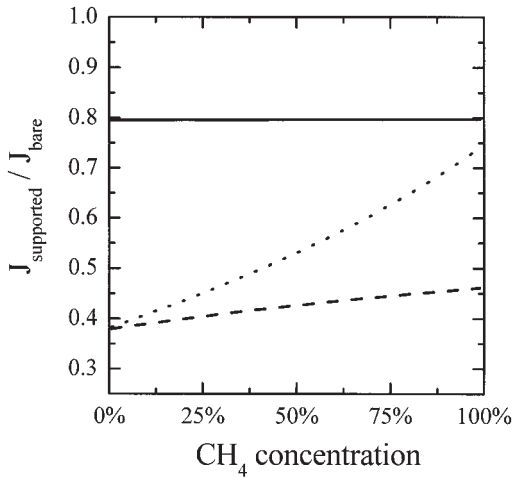

Figure 12. Ratio of CH_4 through supported and unsupported silicalite membranes as a function of the feed composition when there is a total pressure gradient (solid line) and for isobaric conditions for upstream support configuration (dotted line) and downstream support configuration (dashed line).

entations are also much more marked in this regime than in cases of supported membranes with no sweep gas.

The main observations from our calculations are summarized in Figure 12, where the ratio of the flux of CH_4 through supported and unsupported silicalite membranes is plotted as a function of CH_4 concentration in CH_4/He mixtures, at room temperature and for a feed pressure of 296 kPa. When there is a total pressure gradient, the support reduces CH_4 fluxes by about 20%, with or without He as a sweep gas. At a constant total pressure, however, the combined effect of the support and the sweep gas reduces CH_4 fluxes as much as 70% under the conditions studied. For the same conditions, a large difference between a normal and a reverse support placement was observed, especially for CH_4-rich mixtures.

Our results complement those from experiments with zeolite membranes that have systematically studied the impact of operating conditions and sweep gases.[6,7] Experiments of this type have previously provided examples of the impact of membrane orientation and the presence of sweep gases. An advantage of the model used here is that we can additionally compare the outcomes with the intrinsic properties of unsupported membranes, a task that is difficult to accomplish experimentally.

The examples provided here have treated only one permeating species, CH_4, and a single sweep gas, He. Physical intuition suggests that if a larger and more strongly adsorbing gas is used as a sweep gas, then the effects attributed above to the sweep gas will become stronger. One example of this phenomenon can be seen in the experiments of van der Graaf et al.,[6,7] which compared the properties of Ar and He as sweep gases. In all cases studied the major effect of the support and the sweep gas is the reduction of the effective concentration gradient of the diffusing species over the zeolite membrane. For stronger adsorbing species, the Henry's law constant and thus the initial slope of the adsorption isotherm are larger. At those pressure ranges, where the adsorbed amount is increasing rapidly, the effect of the support and the sweep gas are expected to be the largest.

Our calculations have examined randomly oriented polycrystalline zeolite membranes. In this case, it is appropriate to use diffusion coefficients averaged over the crystallographic orientations of silicalite. Exciting experimental progress has been made in the synthesis of supported silicalite membranes with crystals oriented along the *b*-axis.[60] To extend our models to membranes of this type, one would simply replace the orientationally averaged diffusivities with the appropriate directional diffusivity. Diffusion along the *b*-axis of silicalite is slightly faster than the orientationally averaged result, but the two quantities are otherwise similar.[19] As a result, the physical conclusions we have presented for randomly oriented membranes should apply equally to oriented membranes such as those developed by Lai et al.[60]

Acknowledgments

This work was partially supported by the National Science Foundation through Grant CTS-9983467.

Literature Cited

1. Matsukata M, Kikuchi E. Zeolitic membranes: Synthesis, properties and prospects. *Bull Chem Soc Jpn.* 1997;70:2341.
2. Coronas J, Santamaria J. Separations using zeolite membranes. *Sep Purif Methods.* 1999;28:127.
3. Tsapatsis M, Gavalas GR. Synthesis of porous inorganic membranes. *MRS Bull.* 1999;24:30-35.
4. Kärger J, Ruthven D. *Diffusion in Zeolites and Other Microporous Materials.* New York, NY: Wiley; 1992.
5. Chen LG, Falcioni M, Deem MW. Disorder-induced time-dependent diffusion in zeolites. *J Phys Chem B.* 2000;104:6033-6039.
6. van de Graaf JM, Kapteijn F, Moulijn JA. Methodological and operational aspects of permeation measurements on silicalite-1 membranes. *J Membr Sci.* 1998;144:87-104.
7. van de Graaf JM, van der Bijl E, Stol A, Kapteijn F, Moulijn JA. Effect of operating conditions and membrane quality on the separation performance of composite silicalite-1 membranes. *Ind Eng Chem Res.* 1998;37:4071-4083.
8. Bode E, Hoempler C. Transport resistances during pervaporation through a composite membrane: Experiments and model calculations. *J Membr Sci.* 1996;113:43-56.
9. Beuscher U, Gooding CH. Characterization of the porous support layer of composite gas permeation membranes. *J Membr Sci.* 1997;132:213-227.
10. Beuscher U, Gooding CH. The permeation of gas mixtures through support structures of composite membranes. *J Membr Sci.* 1998;150:57-73.
11. Beuscher U, Gooding CH. The influence of the porous support layer of composite membranes on the separation of binary gas mixtures. *J Membr Sci.* 1999;152:99-116.
12. Gump CJ, Lin X, Falconer JL, Noble RD. Experimental configuration and adsorption effects on the permeation of C-4 isomers through ZSM-5 zeolite membranes. *J Membr Sci.* 2000;173:35-52.
13. Talu O, Sun MS, Shah DB. Diffusivities of *n*-alkanes in silicalite by steady-state single-crystal membrane technique. *AIChE J.* 1998;44:681-694.
14. Bowen TC, Falconer JL, Noble RD, Skoulidas AI, Sholl DS. A comparison of atomistic simulations and experimental measurements of light gas permeation through zeolite membranes. *Ind Eng Chem Res.* 2002;41:1641-1650.
15. Skoulidas AI, Bowen TC, Doelling CM, Falconer JL, Noble RD, Sholl DS. Comparing atomistic simulations and experimental measurements for CH_4/CF_4 mixture permeation through silicalite membranes. *J Membr Sci.* 227:123-136, 2003.
16. Skoulidas AI, Ackerman DM, Johnson JK, Sholl DS. Rapid transport of gases in carbon nanotubes. *Phys Rev Lett.* 2002;89:185901.

17. Sholl DS. Predicting single-component permeance through macroscopic zeolite membranes from atomistic simulations. *Ind Eng Chem Res.* 2000;39:3737-3746.
18. Skoulidas AI, Sholl DS. Direct tests of the Darken approximation for molecular diffusion in zeolites using equilibrium molecular dynamics. *J Phys Chem B.* 2001;105:3151-3154.
19. Skoulidas AI, Sholl DS. Transport diffusivities of CH_4, CF_4, He, Ne, Ar, Xe, and SF_6 in silicalite from atomistic simulations. *J Phys Chem B.* 2002;106:5058-5067.
20. Skoulidas AI, Sholl DS. Molecular dynamics simulations of self-diffusivities, corrected diffusivities, and transport diffusivities of light gases in four silica zeolites to assess influences of pore shape and connectivity. *J Phys Chem A.* 2003;107:10132-10141.
21. Schuring D, Koriabkina AO, de Jong AM, Smit B, van Santen A. Adsorption and diffusion of *n*-hexane/2-methylpentane mixtures in zeolite silicalite: Experiments and modeling. *J Phys Chem B.* 2001; 105:7690-7698.
22. Goj A, Sholl DS, Akten ED, Kohen D. Atomistic simulations of CO_2 and N_2 adsorption in silica zeolites: The impact of pore size and shape. *J Phys Chem B.* 2002;106:8367-8375.
23. Heuchel M, Snurr RQ, Buss E. Adsorption of CH_4–CF_4 mixtures in silicalite: Simulation, experiment, theory. *Langmuir.* 1997;13:6795-6804.
24. Lachet V, Boutin A, Tavitian B, Fuchs AH. Molecular simulation of *p*-xylene and *m*-xylene in Y zeolites: Single component and binary mixtures study. *Langmuir.* 1999;15:8678-8685.
25. Yang J-H, Clark LA, Ray GJ, Kim VJ, Du H, Snurr RQ. Siting of mixtures in mordenite zeolites: 19F and 129Xe NMR and molecular simulations. *J Phys Chem B.* 2001;105:4698-4708.
26. Challa SR, Sholl DS, Johnson JK. Adsorption and separation of hydrogen isotopes in carbon nanotubes: Multicomponent grand canonical Monte Carlo simulations. *J Chem Phys.* 2002;116:814-824.
27. Doulsin DR, Harrison RH, Moore RT. Pressure–volume–temperature relations in the system methane–tetrafluoromethane. I. Gas densities and the principle of corresponding states. *J Phys Chem.* 1967;71:3477-3488.
28. Dymond JH, Smith EB. *The Virial Coefficients of Gases—A Critical Compilation.* Oxford, UK: Clarendon Press; 1969.
29. Krishna R, van den Broeke LJP. The Maxwell–Stefan description of mass-transport across zeolite membranes. *Chem Eng J.* 1995;57:155-162.
30. Keil FJ, Krishna R, Coppens MO. Modeling of diffusion in zeolites. *Rev Chem Eng.* 2000;16:71-197.
31. Theodorou DN, Snurr RQ, Bell AT. Molecular dynamics and diffusion in microporous materials. In: Alberti G, Bein T, eds. *Comprehensive Supramolecular Chemistry.* Vol. 7. New York, NY: Pergamon Press; 1996:507-548.
32. Sanborn MJ, Snurr RQ. Predicting membrane flux of CH_4 and CF_4 mixtures in faujasite from molecular simulations. *AIChE J.* 2001;47: 2032-2041.
33. Sanborn MJ, Snurr RQ. Diffusion of binary mixtures of CF_4 and *n*-alkanes in faujasite. *Sep Purif Technol.* 2000;20:1-13.
34. Kärger J. Random walk through two-channel networks: A simple means to correlate the coefficients of anisotropic diffusion in ZSM-5 type zeolites. *J Phys Chem.* 1991;95:5558-5560.
35. Habgood HW. The kinetics of molecular sieve action—Sorption of nitrogen–methane mixtures by Linde molecular sieve 4Å. *Can J Chem.* 1958;36:1384-1397.
36. van de Graaf JM, Kapteijn F, Moulijn JA. Modeling permeation of binary mixtures through zeolite membranes. *AIChE J.* 1999;45:497-511.
37. Yang RT, Chen YD, Yeh YT. Prediction of cross-term coefficients in binary diffusion: Diffusion in zeolite. *Chem Eng Sci.* 1991;46:3089-3099.
38. Krishna R. Diffusion of binary mixtures in zeolites: Molecular dynamics simulations versus Maxwell–Stefan theory. *Chem Phys Lett.* 2000; 326:477-484.
39. Karger J, Bulow M. Theoretical prediction of uptake behavior in adsorption-kinetics of binary gas-mixtures using irreversible thermodynamics. *Chem Eng Sci.* 1975;30:893-896.
40. Kapteijn F, Bakker WJW, Zheng G, Poppe J, Moulijn J. Permeation and separation of light hydrocarbons through a silicalite-1 membrane. Application of the generalized Maxwell–Stefan equations. *Chem Eng J.* 1995;57:145-153.
41. Tuchlenski A, Uchytil P, Seidel-Morgenstern A. An experimental study of combined gas phase and surface diffusion in porous glass. *J Membr Sci.* 1998;140:165-184.
42. Krishna R. Multicomponent surface-diffusion of adsorbed species—A description based on the generalized Maxwell–Stefan equations. *Chem Eng Sci.* 1990;45:1779-1791.
43. Maceiras DB, Sholl DS. Analysis of binary transport diffusivities and self-diffusivities in a lattice model for silicalite. *Langmuir.* 2002;18: 7393-7400.
44. Schiesser WE. *The Numerical Method of Lines: Integration of Partial Differential Equations.* San Diego, CA: Academic Press; 1991.
45. Tuan VA, Falconer JL, Noble RL. Alkali-free ZSM-5 membranes: Preparation conditions and separation performance. *Ind Eng Chem Res.* 1999;38:3635.
46. Datta R, Rinker RG. The flow of rarefied-gases through long tubes of circular cross-section. *Can J Chem Eng.* 1981;59:268-278.
47. Steckelmacher W. Knudsen-flow 75 years on—The current state-of-the-art for flow of rarefied-gases in tubes and systems. *Rep Prog Phys.* 1986;49:1083-1107.
48. Scott DS, Dullien FAL. The flow of rarefied gases. *AIChE J.* 1962;8: 293-297.
49. Scott DS, Dullien FAL. Diffusion of ideal gases in capillaries and porous solids. *AIChE J.* 1962;8:113-117.
50. Pollard WG, Present RD. On gaseous self-diffusion in long capillary tubes. *Phys Rev.* 1948;73:762-774.
51. Present RD, Pollard WG. On the self-diffusion of a pure gas through a long capillary when the mean free path is comparable to the capillary diameter. *Phys Rev.* 1946;69:53-53.
52. Lund LM, Berman AS. Flow and self-diffusion of gases in capillaries. 2. *J Appl Phys.* 1966;37:2496-2503.
53. Lund LM, Berman AS. Flow and self-diffusion of Gases in capillaries. 1. *J Appl Phys.* 1966;37:2489-2495.
54. Reid RC, Prausnitz JM, Poling BE. *Properties of Gases and Liquids.* New York, NY: McGraw-Hill; 1987.
55. Chung TH, Ajlan M, Lee LL, Starling KE. Generalized multiparameter correlation for nonpolar and polar fluid transport properties. *Ind Eng Chem Res.* 1988;27:671-679.
56. Bhatia SK, Jepps O, Nicholson D. Tractable molecular theory of transport of Lennard Jones fluids in nanopores. *J Chem Phys.* 2004; 120:4472-4485.
57. Mason EA, Malinaus.Ap, Evans RB. Flow and diffusion of gases in porous media. *J Chem Phys.* 1967;46:3199.
58. Mason EA, Malinauskas AP. *Gas Transport in Porous Media: The Dusty-Gas Model.* Amsterdam/New York, NY: Elsevier; 1983.
59. Fuller EN, Ensley K, Giddings JC. Diffusion of halogenated hydrocarbons in helium. Effect of structure on collision cross sections. *J Phys Chem.* 1969;73:3679.
60. Lai Z, Bonilla G, Diaz I, Nery JG, Sujaoti K, Amut MA, Kokkoli E, Terasaki O, Thompson RW, Tsapatsis M, Vlachos DG. Microstructural optimization of a zeolite membrane for organic vapor separation. *Science.* 2003;300:456-460.

Manuscript received May 12, 2004, and revision received Jun. 30, 2004.